Transactions of Tianjin University (2021) 27:280–294
https://doi.org/10.1007/s12209-021-00290-y

REVIEW

Photocatalytic Synthesis of High-Energy-Density Fuel: Catalysts, Mechanisms, and Challenges

Jie Xiao[1,2] · Jiaxiang Zhang[1,2] · Lun Pan[1,2] · Chengxiang Shi[1,2] · Xiangwen Zhang[1,2] · Ji-Jun Zou[1,2]

Received: 26 March 2021 / Revised: 6 April 2021 / Accepted: 16 April 2021 / Published online: 2 June 2021

Abstract

High-energy-density liquid hydrocarbon fuels are generally synthesized using various chemical reactions to improve the performance (e.g., range, load, speed) of aerospace vehicles. Compared with conventional fuels, such as aviation kerosene and rocket kerosene, these liquid hydrocarbon fuels possess the advantages of high-energy-density and high volumetric calorific value; therefore, the fuels have important application value. The photocatalytic process has shown great potential for the synthesis of a diverse range of fuels on account of its unique properties, which include good efficiency, clean atomic economy, and low energy consumption. These characteristics have led to the emergence of the photocatalytic process as a promising complement and alternative to traditional thermocatalytic reactions for fuel synthesis. Extensive effort has been made toward the construction of catalysts for the multiple photocatalytic syntheses of high-energy-density fuels. In this review, we aim to summarize the research progress on the photocatalytic synthesis of high-energy-density fuel by using homogeneous and heterogeneous catalytic reactions. Specifically, the synthesis routes, catalysts, mechanistic features, and future challenges for the photocatalytic synthesis of high-energy-density fuel are described in detail. The highlights of this review not only promote the development of the photocatalytic synthesis of high-energy-density fuel but also expand the applications of photocatalysis to other fields.

Graphic abstract

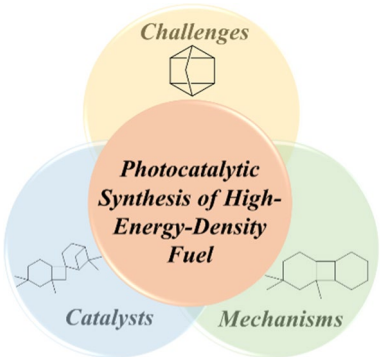

Keywords High-energy-density fuel · Photocatalysis · Cycloaddition · Catalyst · Mechanism

✉ Chengxiang Shi
cxshi@tju.edu.cn

✉ Ji-Jun Zou
jj_zou@tju.edu.cn

[1] Key Laboratory for Green Chemical Technology of Ministry of Education, School of Chemical Engineering and Technology, Tianjin University, Tianjin 300072, China

[2] Collaborative Innovative Center of Chemical Science and Engineering (Tianjin), Tianjin 300072, China

Introduction

Continuous improvements in modern aircraft technology have resulted in more stringent requirements for the liquid propellants used in various aircraft. When the volume of the fuel tank is limited, fuel with higher density and volumetric calorific value can provide more energy for

the aircraft than conventional fuels, thereby improving the speed and range of the vehicle. Synthetic high-energy-density hydrocarbon compound is an important liquid fuel that can meet the energy requirements of various aircrafts. Thus, this type of fuel has attracted increased attention from the scientific community.

The properties of hydrocarbon fuels are mainly determined by their molecular framework, which includes linear, branched, and cyclic structures, and spatial configurations, such as bridged and hanging or *cis*- and *trans*-isomers. In general, the density of chain alkane fuels is lower than those of polycyclic and caged paraffinic fuels. High-energy-density polycyclic hydrocarbon compounds are generally produced in liquid form; these compounds have a high density and heat of combustion and suitable flash point and melting point, which means they can usually be burned directly as fuel. The density and heat of combustion of high-energy-density caged hydrocarbon compounds are much higher than those of conventional paraffinic fuels. However, because high-energy-density cage-like compounds usually have high melting points and exist in solid form, their combustion rate cannot be controlled, and they are inconvenient to use directly. Therefore, these compounds are often dissolved in high-energy-density polycyclic hydrocarbon fuels to obtain a compounded fuel with improved overall combustion performance.

Traditional high-energy-density hydrocarbon fuels are mostly prepared through cycloaddition, hydrogenation, and skeletal isomerization under harsh, energy-intensive conditions. Given the increasing severity of the environmental crisis, the urgency of sustainable development has been highlighted, and the conversion of renewable energy to produce high-energy-density hydrocarbon fuels has gradually become an important research focus [1]. Photocatalysis utilizes renewable solar energy to achieve high efficiency, clean atomic economy, and low energy consumption under low-toxic and even non-toxic conditions [2, 3]. Interestingly, the [2 + 2] cycloaddition of olefins, which provides a versatile and straightforward approach to construct high-energy-density polycyclic fuels, is thermally forbidden but can be achieved by photochemical activation [4].

Reports on the synthesis of high-energy-density fuel using thermocatalytic methods have been well reviewed [5, 6], but comprehensive reviews on the photocatalytic synthesis of high-energy-density fuels are lacking. Herein, we review the research progress on high-energy-density fuel synthesis via the photocatalytic process and describe future perspectives and remaining challenges. It is hoped that this review could facilitate the rational design and construction of new high-energy-density fuels for aerospace propulsion.

Homogeneous Photocatalytic Synthesis

Homogeneous molecular photocatalysts, such as transition metal complexes and ketone-based molecular catalysts, were introduced in earlier research on photoinduced high-energy-density fuel synthesis. Homogeneous photocatalysts possess excellent activity, high selectivity, and well-defined active sites to promote the catalytic reaction. This section describes the homogeneous photocatalytic synthesis via the metal-based/ketone-based molecular catalysts and the self-sensitization reaction.

Synthesis of Quadricyclane with Metal- and Ketone-Based Molecular Catalysts

Quadricyclane (QC, tetracyclo[3.2.0.0^{2,7}.0^{4,6}]heptane) molecular contains two three-membered rings, one four-membered ring, and two five-membered ring structures, all of which combine to form a strained and caged hydrocarbon with a high density of 0.982 g/cm^3. The bond angles in the three- and four-membered rings are in the range of 59.9°–90.0°, much smaller than the usual bond angle of 109.5°. The net heat of combustion of this strained and caged structure is 44.35 MJ/kg, which is much higher than that of the high-energy fuel JP-10 (i.e., 42.10 MJ/kg). QC possesses good low-temperature properties (e.g., − 40 °C viscosity: 0.03 Pa·s) and, thus, is a very promising high-energy-density fuel. QC is generally synthesized via the photoisomerization of norbornadiene (NBD, [2.2.1]-bicycloheptadiene). Some photocatalysts used to synthesize QC are summarized in Table 1.

In fact, since NBD can only absorb ultraviolet light (ca. 230 nm), obtaining QC by the direct photoinduced valence isomerization of this compound is difficult. Photosensitizers can be used to increase the efficiency of isomerization and utilize long-wavelength visible light. Homogeneous photosensitizers can be categorized as triplet sensitizers and transition metal compound-based sensitizers. The triplet state energy (E_T) of NBD is ca. 257 kJ/mol, which is fairly high, and only a few sensitizers with E_T higher than 257 kJ/mol can satisfy the classical triplet–triplet transfer process.

In the triplet sensitization mechanism, the sensitizer first absorbs photons, transitions to the singlet state, and then transitions to the triplet state ^{3}S through inter-system crossing [7], as shown in Fig. 1a. The E_T is transferred from ^{3}S to the ground-state NBD molecules to generate energetic ^{3}NBD, which is then adiabatically isomerized to ^{3}QC and relaxed to the ground-state QC.

Hammond et al. [8] demonstrated that the photoisomerization of NBD could be accomplished by triplet sensitizers

Table 1 Catalysts and their photocatalytic activity for the photoisomerization of NBD to QC

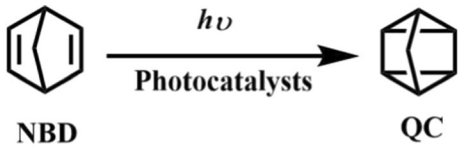

Entry	Catalysts	Time (h)	Yield (%)	Ref
1	Acetophenone	6	100	8
2	Benzophenone	6	86	8
3	Diethyl Michler's ketone	1	~85	11
4	Michler's ketone	1	~55	11
5	4,4′-Diaminobenzophenone	1	~45	11
6	3,3′-4,4′-Benzophenonetetracarboxylic dianhydride	1	~5	11
7	$Rh(phen)_3^{3+}$ (phen = 1,10-phenanthroline)	–	76	15
8	ZnO/ZnS/CdS	28–30	90–100[a]	29
9	1% Zn/TiO_2	5	~75	38
10	V-doped Ti^{3+}-TiO_2/MCM-41	3	~80[a]	41
11	Tl^+ exchanged Y-zeolites	3	90	43
12	La-exchanged Y-zeolites	7	~80[a]	45
13	Ti-MCM-41	12	90	47
14	V-Ti-MCM-41	4	85	48

[a]Conversion

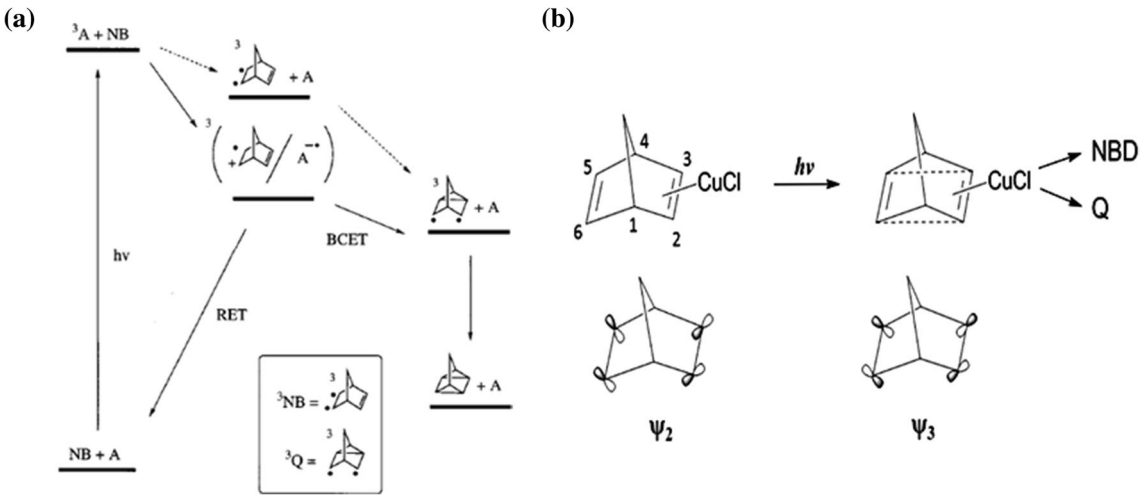

Fig. 1 **a** Mechanism of triplet sensitization valence isomerization of norbornadiene (NBD) to quadricyclane (QC). BCET, bond-coupled electron transfer; RET, return electron transfer. Reproduced with permission from Ref. [7]. Copyright 1999 American Chemical Society. **b** Proposed mechanism of the CuCl photoassisted isomerization of NBD to QC and representation of the highest filled (ψ_2) and lowest unfilled (ψ_3) π molecular orbitals on NBD. Reproduced with permission from Ref. [14]. Copyright 1977 American Chemical Society

such as benzophenone or acetophenone. Researchers have explored a large number of photosensitizers for isomerization, including organic compounds containing carbonyl groups, such as propiophenone, benzophenone, acridinone, and Michler's ketone [9, 10]. Among these sensitizers, Michler's ketone, acetophenone, and benzophenone demonstrated the best effectiveness. Given the small difference in E_T between these compounds and NBD, the temperature does not remarkably influence the performance of acetophenone and benzophenone but greatly affects that of Michler's ketone. A quenching experiment was performed with piperylene or 2,5-dimethyl-2,4-hexadiene

as the quencher, and results indicated that triplet excitation is transferred from the ketones to NBD with a rate constant of approximately 10^9 L/(mol·s). The initial products of excitation transfer to NBD either have lifetimes of less than 1 ns or are converted almost completely to QC, regardless of whether they undergo self-decay or whether they decay by interaction with quencher.

Su et al. [11] designed a simple and inexpensive UV-LED-based photomicroreactor assembly using commercially available components for the photoisomerization of NBD to QC and then optimized the type and concentration of photosensitizers, solvents, and light sources for this photochemical process. A series of triplet photosensitizers, such as Michler's ketone (4,4′-diaminobenzophenone), diethyl Michler's ketone, and 3,3′-4,4′-benzophenonetetracarboxylic dianhydride, were selected for photosensitization. Among these sensitizers, diethyl Michler's ketone proved to be the most suitable photosensitizer for the NBD/QC system because of the overlap of the π–π* absorption band of this reagent with the UV-LED emission spectrum, which resulted in high QC yield. The type of solvent used plays an important role not only in the absorption shift of diethyl Michler's ketone but also in the yield of the final product. The use of dichloromethane or acetone leads to better photochemical properties compared with those produced by other solvents. UV-LED strips show certain advantages over traditional high-pressure mercury lamps in terms of cost, service life, and photocatalytic performance, thus supporting the potential role of UV-LEDs in the field of photochemical organic conversion.

Difficulties in developing new systems with high E_T and the formation of by-products, such as the polymerization of NBD, in recent years, have limited the application of triplet sensitizers in photoisomerization. Therefore, researchers have sought to develop sensitizers based on transition metal compounds as an alternative to triplet sensitizers [12]. Trecker et al. [13] confirmed that cuprous halide catalyzes the photodimerization of norbornene, and quantum yield measurements showed that the relevant reaction mechanism involves the attack of the light-excited norbornene–cuprous halide complex on the two uncomplexed ground states of norbornene. Schwendiman and Kutal [14] applied CuCl to the photoinduced isomerization of NBD to QC and obtained very high quantum yields of photoisomerization ranging from 0.3 to 0.4 in chloroform and from 0.2 to 0.3 in ethanol at 313 nm. The conversion rate of NBD could exceed 90%. In addition, the photoreaction revealed a clear solvent dependence: Isomerization was conducted efficiently in $CHCl_3$ and C_2H_5OH, but no detectable conversion occurred in CH_3CN.

The mechanism of CuCl photoinduced NBD conversion is shown in Fig. 1b. First, light irradiation at 313 nm induces charge transfer, which generates the excited state of the ClCu-NBD π complex. The 3d electrons of Cu^I are transferred to the lowest unoccupied π molecular orbital (ψ_3) of NBD, and the electrons from the highest occupied π molecular orbital (ψ_2) of NBD are transferred to Cu^I. Both cases can weaken C_2–C_3 and C_5–C_6, and strengthen C_2–C_6 and C_3–C_5. The electronically excited complex may split between the relaxation pathways, leading to NBD and QC. It was important that NBD dimers were not produced during the photoreaction process because a single coordination site on the metal [Cu(I)] could effectively inhibit these dimers.

Other transition metal compound-based sensitizers, such as L_3CuX (L = Ph_3P, $MePh_2P$; X = Cl, Br, I), Cu(I)-based dinuclear complexes [Cu_2L_2(μ-NBD), where L = 2-methyl-8-oxoquinolinato, 2-methyl-5,7-dichloro-8-oxoquinolinato, 4-oxoacridinato, 2-(2-oxo-3,5-di-tert-butyl phenyl)benzotriazole], and orthometalated complex (2,2′-bipyrid-3-yl-C^3,N′)bis(2,2-bipyridine-N,N′)iridium(III) and Rh(III) diimine complexes [$Rh(phen)_3^{3+}$ and $Rh(phi)_2(phen)^{3+}$ (phen = 1,10-phenanthroline, phi = 9,10-phenanthrenequinone diimine)], have been applied to the photoisomerization of NBD to QC [15–17]. Sensitizers containing complex ligands have a broad light absorption range extending to the visible light region and improved utilization efficiency for sunlight, but their high cost limits their practical applications. Some metal complexes, including carboxamide and sulfonamide-linked polystyrene anchored cobalt(II) tetraarylporphyrin, are also highly active photocatalysts for converting NBD to QC. Unfortunately, cobalt complex catalysts are gradually deactivated by partial oxidation during the reaction; the activity of these catalysts can be partially restored by treatment with a strong reducing agent, such as Ti^{3+}.

The aforementioned metal- and ketone-based molecular catalysts are, in essence, homogeneous catalysts and, therefore, possess the common drawbacks of homogeneous catalysts, including difficult separation from the product and recovery. Thus, the development of heterogeneous catalysts with the unique structural features of homogeneous catalysts but without the associated problems of the latter is highly desired.

Synthesis of Spiro- and Cage-Fuels by the Self-Sensitization Reaction

Spiro-Fuels

Spirocyclic molecules have two-ring structures that share a carbon atom. Because their molecular structure is compact, spirocyclic alkanes have a fairly high density. More importantly, spirocycloalkanes have good low-temperature properties. For example, the freezing point of spiro[2,2] pentane has been reported to be as low as − 107 °C. Therefore, spirocyclic alkanes represent high-energy-density

fuel molecules with great application potential. In general, spirocyclic alkanes can be constructed by the Lewis acid-catalyzed rearrangement of pinacol, cyclization of halogen-substituted cyclic ketones with organic bimetallic reagents, or cyclization of 1,6-dienes with Grignard reagents. However, these methods require expensive reagents, are sensitive to air, include complicated operations, and are generally unsuitable for large-scale production. Compared with thermocatalytic reactions, photocatalytic reactions feature relatively milder conditions and, in many cases, have higher selectivity.

Zou's group [18] synthesized spiro-fuel through a photoinduced self-sensitized [2 + 2] cycloaddition and hydrodeoxygenation process. Biomass-derived β-pinene and isophorone with no extra photosensitizer were irradiated under a high-pressure mercury lamp for 9 h; here, isophorone functions not only as a reactant but also as a photosensitizer because of the carbonyl group in its molecular structure. The cycloaddition mechanism of isophorone

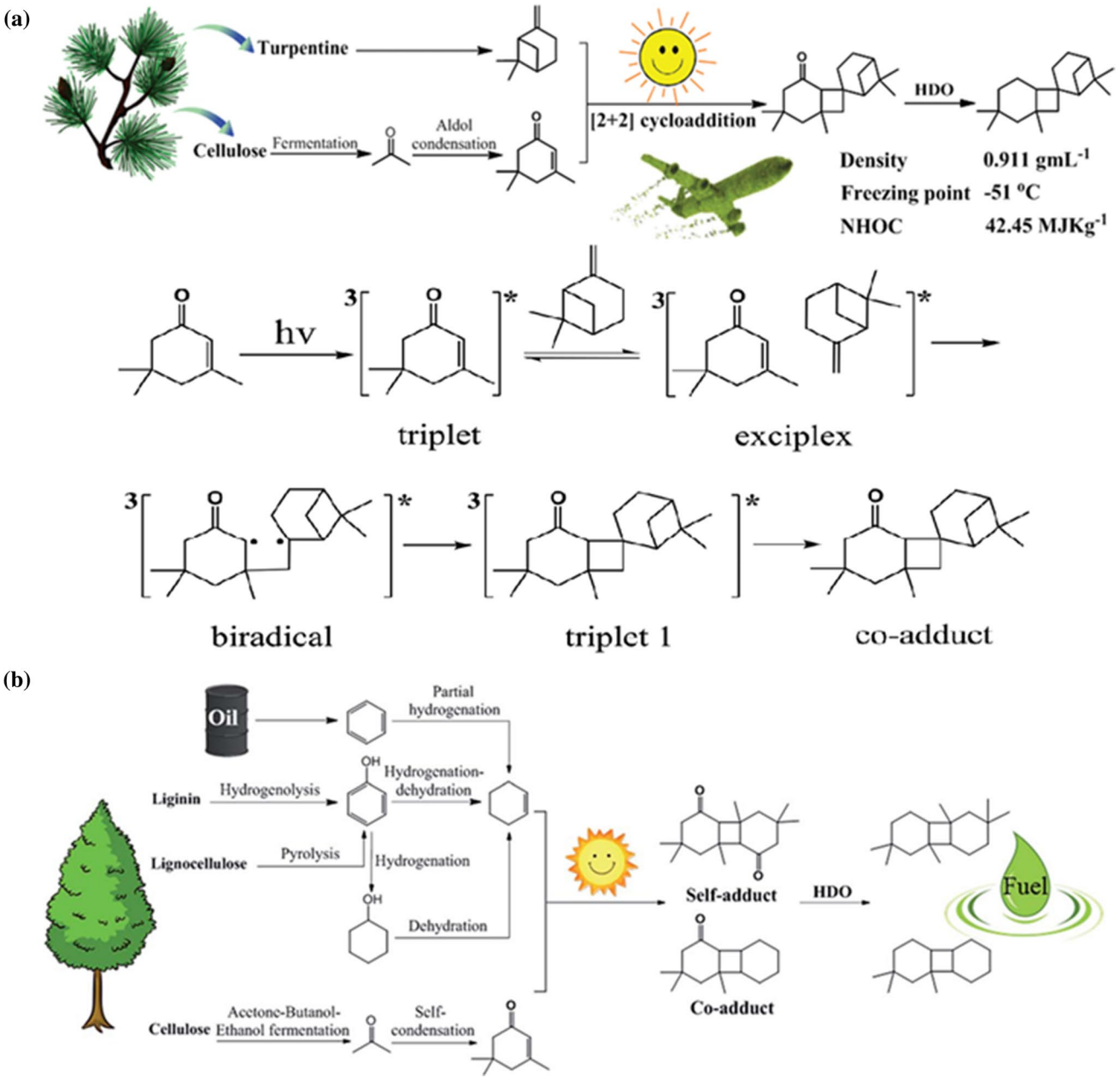

Fig. 2 **a** Whole synthesis scheme of biomass-derived spiro-fuel. Reproduced with permission from Ref. [18]. Copyright 2019 Royal Society of Chemistry. **b** Designed route for the self-photosensitized [2 + 2] cycloaddition synthesis of high-energy-density hydrocarbons. Reproduced with permission from Ref. [19]. Copyright 2020 Royal Society of Chemistry

and β-pinene may involve a self-sensitized triplet energy transfer process, as shown in Fig. 2a. Under light irradiation, the isophorone molecule is excited to form a triplet state by absorbing photon energy. Triplet isophorone then collides with ground-state *β*-pinene to form an active complex and decays into triplet 1 of the target product through the high-energy triplet biradical intermediate. Triplet 1 is subsequently transformed into the target copolymer adduct through the transition of the band gap energy level. The optimal molar ratio of isophorone to β-pinene has been evaluated, and the desired co-adduct could be achieved in 95.1% conversion and 91.1% yield under an optimal molar ratio of 1:4. Further increases molar ratio may induce self-cycloaddition and inhibit co-cycloaddition. The co-adduct could be hydrodeoxygenated to saturated spiro-fuel in 85.0% overall yield by the bifunctional catalyst Pt/HY in H_2. Metal platinum can promote hydrogenation, and the acidic support HY can catalyze dehydration. The saturated co-adduct spiro-fuel has a density of 0.911 g/mL, a volumetric net heat of combustion of 38.67 MJ/L, a freezing point of − 51 °C, and kinematic viscosity of 176 mm^2/s at − 20 °C.

The same group then used biomass-derived ketenes (isophorone) and olefins (cyclohexene) as a reactant without extra photosensitizers or photocatalysts to prepare high-tension four-membered ring high-energy-density fuels via self-sensitized [2 + 2] cycloaddition (Fig. 2b) [19]. In this reaction, isophorone functions as both a sensitizer and reactant in the reaction; triplet isophorone is the key to initiating the photoreaction, and the large E_T gap between the quencher and isophorone can enhance the efficiency of triplet energy transfer. Compared with the self-polycycloaddition of isophorone, the isophorone/cyclohexene copolymerization cycloaddition reaction has lower activation energy, higher conversion rate, and higher quantum yield. The quantum yield (365 nm) of the cycloaddition reaction of isophorone and cyclohexene is as high as 88.3%. The cycloaddition product could be converted into a four-membered ring hydrocarbon fuel with high tension through hydrodeoxygenation. This fuel has a higher density and mass calorific value compared with hydrocarbon alkanes produced by the conventional C–C coupling method. In particular, the four-membered ring fuel densities obtained from the copolymerized cycloaddition product and the self-polymerized cycloaddition product were 0.903 and 0.892 g/mL, respectively.

The thermally forbidden resistance of [2 + 2] cyclization in the photocatalytic [2 + 2] reaction could be overcome by using biomass-derived ketene, which acts not only as a reactant but also as a high efficiency photosensitizer to promote the desired reaction. This self-sensitized cycloaddition strategy can be extended to include a wide range of biomass-derived α, β-unsaturated ketones and alkenes.

Cage-Fuels

The pentacyclo[5.4.0.$0^{2,6}$.$0^{3,10}$.$0^{5,9}$]undecane (PCU) molecule contains one four-membered ring and four five-membered rings arranged in a compact cage structure. This compound has a density of 1.239 g/cm^3 and a heat of combustion of 389.0 kJ/mol; thus, it is an ideal candidate for high-energy fuel additives.

Because of the existence of high-tension energy in the molecule, once a certain bond in PCU is broken during the combustion process, the whole molecule rapidly dissociates to release a large amount of energy. Therefore, this compound has very good application prospects in the high-energy fuel field. The tension energy of PCU is much higher than those of ordinary cyclic compounds. The tension energies of typical cyclic compounds, such as boat cyclohexane and cyclopentane, are 6.0 and 30.6 kJ/mol, respectively. The tension energy of cage compounds, such as adamantane, is 28.9 kJ/mol. By comparison, the tension energy of PCU is 343.7 kJ/mol. Research has shown that tension energy is converted into heat energy during combustion, and 5.6% of the combustion heat of PCU (42.0 kJ/g) may be attributed to its tension energy. This high-tension energy is also one of the main reasons behind the high combustion heat of PCU-based compounds.

Marchand and Allen [20] reported the synthesis of PCU, as shown in Fig. 3a. First, the Diels–Alder reaction is performed using cyclopentadiene and *p*-benzoquinone as reactants to obtain brown crystals with a yield of 93%. Then, a medium-pressure mercury lamp is used as a light source to convert crystal *a* into *b* via photocatalytic [2 + 2] addition. Finally, hydrazine hydrodeoxygenation is performed under alkaline conditions to form colorless waxy solid PCU with a yield of 59%. Although PCU has high density, it is volatile, which hinders its direct application.

Singh et al. [21] synthesized pentacyclo[5.4.0.$0^{2,6}$.$0^{3,10}$.$0^{5,9}$]undecane-8,11-dione-4-spiro-1-cyclopropane 2 with a yield of 57.4% (Fig. 3b). First, spiro[4.2]heptadiene undergoes Diels–Alder cycloaddition to react with *p*-benzoquinone dissolved in CTAB micelles to form adduct 1 in 66.0% yield. Thereafter, adduct 1 is converted into solid pentacyclic[5.4.0.$0^{2,6}$.$0^{3,10}$.$0^{5,9}$]undecane-8,11-dione-4-spiro-1-cyclopropane 2 in ethyl acetate solution under UV light irradiation (87.0% yield). Because the reactants in the core of the CTAB micellar pseudophase are ordered in a regular manner, cycloaddition proceeds smoothly. The above-mentioned molecule 2 possesses cyclopropane and cage-like structures, and the saturated hydrocarbons obtained after hydrodeoxygenation may have high net heat of combustion and density.

Shi et al. [22] designed and synthesized double-cage hydrocarbon PCU dimer (Fig. 3c) with a novel structure. The construction of this double-cage structure is directly

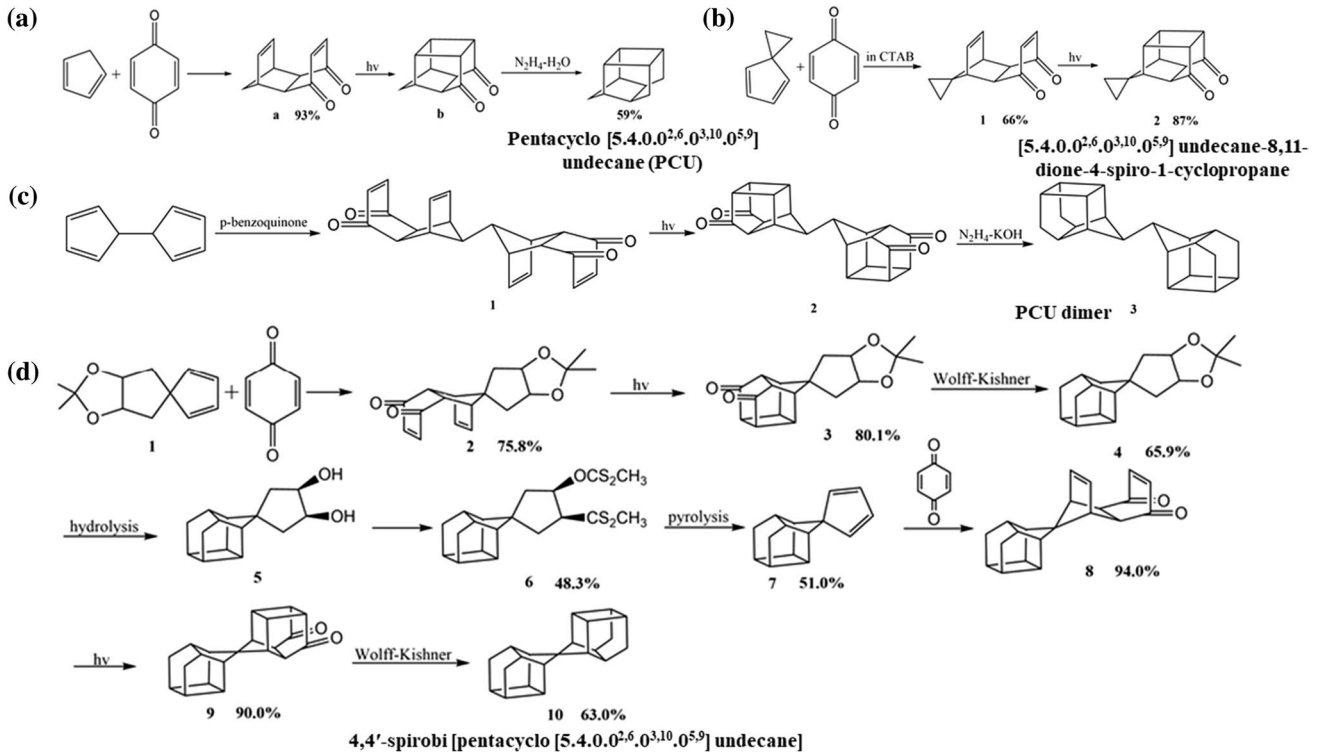

Fig. 3 **a** Synthesis route of PCU. Reproduced with permission from Ref. [20]. Copyright 1974 American Chemical Society. **b** Synthesis route of pentacyclo[5.4.0.0^{2,6}.0^{3,10}.0^{5,9}]undecane-8,11-dione-4-spiro-1-cyclopropane. Reproduced with permission from Ref. [49]. Copyright 2020 John Wiley and Sons. **c** Synthesis route of the double-cage hydrocarbon $C_{22}H_{24}$. Reproduced with permission from Ref. [22]. Copyright 2017 Elsevier. **d** Total synthesis scheme of 4,4′-spirobi[pentacyclo[5.4.0.0^{2,6}.0^{3,10}.0^{5,9}]undecane]. Reproduced with permission from Ref. [23]. Copyright 2015 Elsevier

completed via the Diels–Alder reaction (60% yield) and photocatalytic intramolecular [2 + 2] cycloaddition (85% yield) using 5,5′-bi(cyclopentadiene) and *p*-benzoquinone as the initial reactants with a medium-pressure mercury immersion lamp. Wolff–Kishner reduction (45% yield) is subsequently employed to obtain the PCU dimer. Crystal structural analysis revealed that the structure of the PCU dimer is formed by C–C single bonds. This synthetic route completely avoids the McMurry coupling reaction to connect two single-cage skeleton structures, thereby greatly reducing the synthesis cost of double-cage hydrocarbons. The density of 3 is approximately 1.23 g/cm^3, and its volumetric heat of combustion is 51.67 MJ/L.

Shi et al. [23] designed a nine-step synthetic route to obtain 4,4′-spirobi[pentacyclo[5.4.0.0^{2,6}.0^{3,10}.0^{5,9}]undecane] (Fig. 3d). First, the construction of a cage-like skeleton structure is achieved by using diene 1 and *p*-benzoquinone as initial reactants to obtain a new structure of diene 2, which is then combined with *p*-benzoquinone once more. The Diels–Alder reaction and photocatalytic intramolecular [2 + 2] cycloaddition, and Wolff–Kishner reduction are subsequently conducted to complete the construction of spiro double-cage structure, i.e., 4,4′-spirobi[pentacyclo[5.4.0.0^{2,6}.0^{3,10}.0^{5,9}]undecane]. Analysis of the crystal structure of the product revealed that the structure of 4,4′-spirobi[pentacyclo[5.4.0.02,6.03,10.05,9]undecane] closely resembles those of two PCUs connected through the spiro carbon atom. The product has a density of 1.27 g/cm^3 and volumetric heat of combustion of 53.35 MJ/L; these values are 29.5% and 22.5% higher than those of quadricyclane, respectively.

Underwood and Ramamoorthy [24] reported the synthesis of hexacyclo[5.4.0.0^{2,6}.0^{3,10}.0^{5,9}.0^{8,11}]undecane, also known as homopentaerythrene (Fig. 4a). The Diels–Alder reaction of cyclopentadiene and *p*-benzoquinone is performed to obtain diene-diketone 1 as a solid. Diene-diketone 1 is then subjected to intramolecular [2 + 2] photocyclization to obtain caged dione 2. The yield of diol 3 from the reduction of the dione with lithium aluminum hydride was 70%. Liquid dibromide 4 can be synthesized by bromination with PBr_3 (60% yield), and the target product hexacyclo[5.4.0.0^{2,6}.0^{3,10}.0^{5,9}.0^{8,11}]undecane 5 can be obtained as a white volatile solid (62% yield) by refluxing in ethanol under the smooth catalysis of zinc powder for debromination. Because homopentaprismane is also a volatile solid at room temperature, methylation of this compound can decrease its

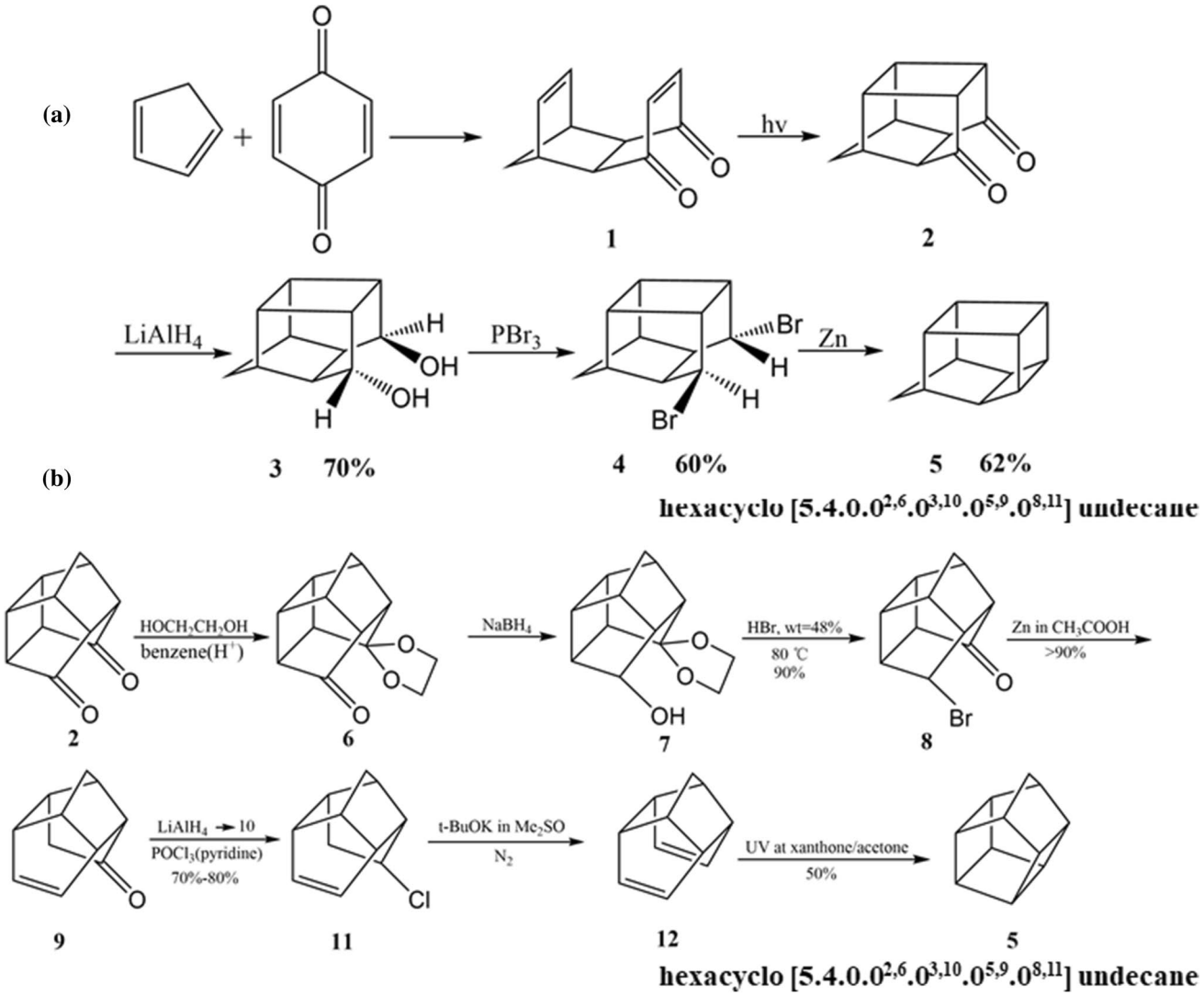

Fig. 4 Synthesis route of hexacyclo[5.4.0.$0^{2,6}$.$0^{3,10}$.$0^{5,9}$.$0^{8,11}$]undecane. Reproduced with permission from Ref. [25]. Copyright 1976 American Chemical Society

melting point and volatility, thereby allowing its utilization as a high-energy additive for conventional aviation kerosene to increase the volumetric net heat of combustion, similar to MPCU. Eaton et al. [25] also reported the synthesis of hexacyclo[5.4.0.$0^{2,6}$.$0^{3,10}$.$0^{5,9}$.$0^{8,11}$]undecane 5 from compound 2 (Fig. 4b). The synthetic route shown in Fig. 4a is clearly simpler and more efficient than that in Fig. 4b.

Cubane is a single-cage hydrocarbon with the highest density (1.29 g/cm^3) and volumetric combustion heat (59.9 MJ/L) developed to date. The structure of cubane is unique because the angle between C–C bonds is 90°; thus, the molecule has a very high-tension energy of 693.9 kJ/mol. The gravimetric net heat of combustion of cubane is approximately 46.5 MJ/kg. The activation energy of cubane decomposition in the gas phase is approximately 180 kJ/mol at 230–260 °C, which means it is inert to air, water, light, and most common reagents and stable at room temperature and atmospheric pressure. Eaton [26] reported the synthesis of cubane via the decomposition of diester 1 (Fig. 5a). In this procedure, diester 1 is obtained from the esterification of cubane-l,4-dicarboxylic acid and cubane-l,4-dicarboxylic acid, which can be synthesized through the cycloaddition of 2 (Fig. 5b).

Gleiter and Karcher [27] reported the synthesis of propella[3_4]prismane 1, as shown in Fig. 5c. Heptacyclo[10.8.0.0^{2,6}.0^{2,11}.0^{6,17}.0^{7,11}.0^{7,16}]icosa-1,16-diene, as a starting material, can be converted from superphane 2 to diene 3 with Ce^{4+} via simple oxidation (70% yield). Then, propella[3_4]prismane 1 can be synthesized from diene 3 (~7% yield) through intramolecular [2+2] photocycloaddition with a 500 W high-pressure mercury lamp. This reaction is reversible under trace acid conditions.

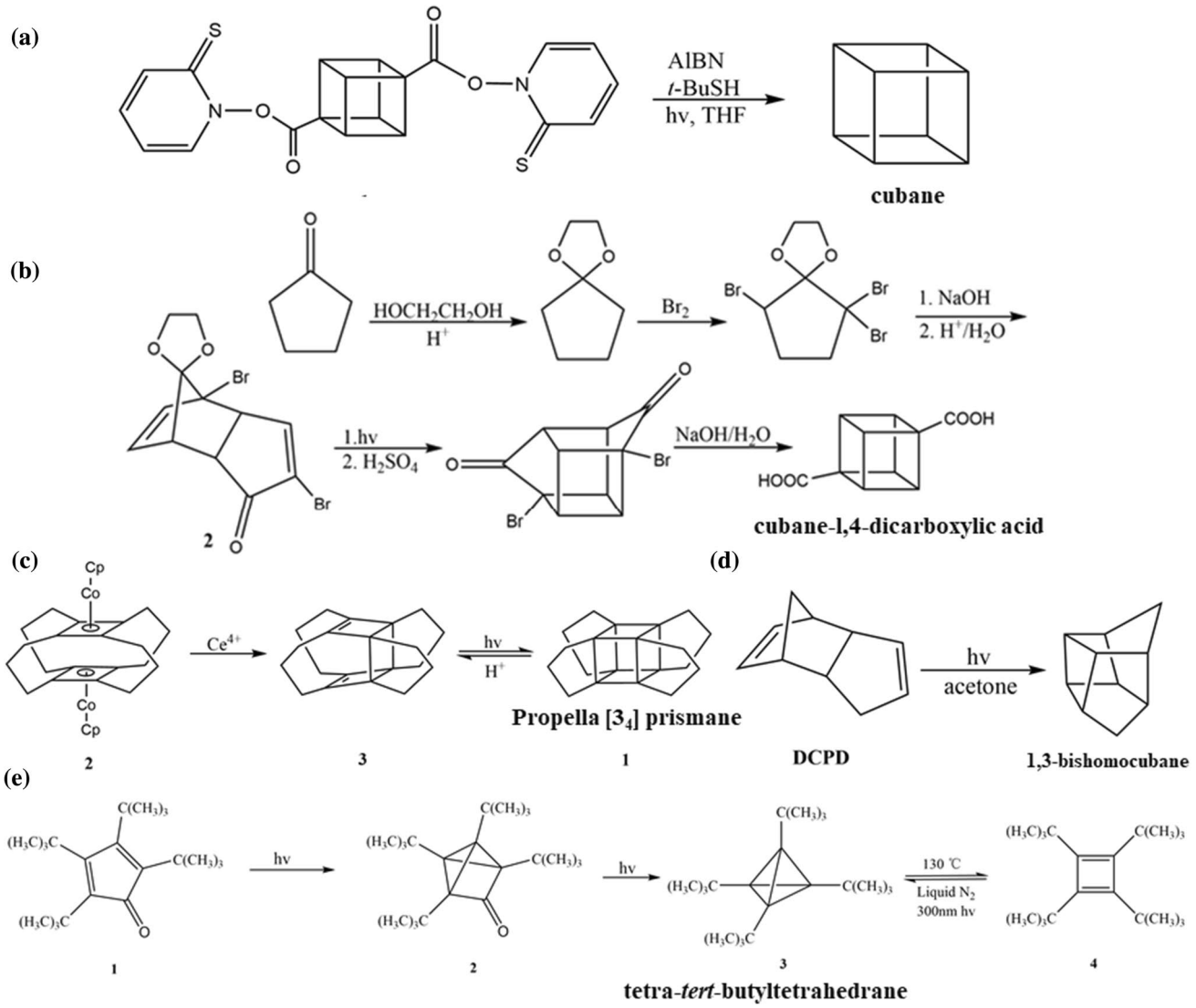

Fig. 5 **a** Decomposition of diester to synthesize cubane. **b** Synthesis of cubane-l,4-dicarboxylic acid. **a** and **b** are reproduced with permission from Ref. [26]. Copyright 1992 John Wiley and Sons. **c** Synthesis scheme of propella[3_4]prismane 1. Reproduced with permission from Ref. [27]. Copyright 1988 John Wiley and Sons. **d** Photocyclization of dicyclopentadiene to form 1,3-bishomocubane. Reproduced with permission from Ref. [49]. Copyright 2020 John Wiley and Sons. **e** Ultraviolet radiation of tetra-*tert*-butylcyclopentadienone to synthesize tetra-*tert*-butyltetrahedrane 3. Reproduced with permission from Ref. [26]. Copyright 1978 John Wiley and Sons

Pentacyclic[5.3.0.$0^{2,5}$.$0^{3,9}$.$0^{4,8}$]decane(1,3-bishomocubane) can be synthesized through the intramolecular [2 + 2] photocyclization of dicyclopentadiene (DCPD) with acetone as a photosensitizer (99.1% yield) (Fig. 5d). The band gap of acetone is narrower than that of DCPD. Thus, acetone can easily absorb UV light to jump to the triplet state and then transfer energy to DCPD, thereby producing an excited intermediate and promoting the [2 + 2] photocyclization reaction. 1,3-Bishomocubane has a mass heat of combustion of 45.2 MJ/kg and melting point of 141.9 °C. When the mass fraction of 1,3-bishomocubane in RP-3 is 50%, the density and volumetric heat of combustion of the resulting mixed fuel are 0.91 g/cm^3 and 43.50 MJ/L, respectively; these values are approximately 15% higher than those of pure RP-3. Such findings indicate that 1,3-bishomocubane is an excellent additive with broad application prospects.

Maier et al. [28] reported the synthesis of tetra-*tert*-butyltetrahedrane (Fig. 5e). Tetra-*tert*-butyltetrahedrane 3 can be obtained from tetra-*tert*-butylcyclopentadienone under UV light irradiation (254 nm) (35% yield, 77 h). 3 can also be converted back to tetra-*tert*-butylcyclobutadiene 4 at 130 °C via quantitative isomerization. Tetra-*tert*-butyltetrahedrane 3 is a colorless soft needlelike solid with a melting temperature of 135 °C and a strain energy higher than that of QC (560.7 kJ/mol vs. 392.9 kJ/mol).

Heterogeneous Photocatalytic Synthesis

Homogeneous molecular photocatalysts, such as transition metal complexes and organic dyes, provide excellent activity, high selectivity, and numerous active sites during homogeneous photocatalytic fuel synthesis, but they are expensive, difficult to separate from the reaction system, and have low recycling efficiency. Considering their easy purification from the product and favorable recyclability, heterogeneous photocatalysts are also considered attractive materials for photocatalytic fuel synthesis. Therefore, the design and construction of inexpensive and environment-friendly heterogeneous photocatalysts for photocatalytic fuel synthesis are highly desired. In this section, we focus on the heterogeneous photocatalytic synthesis via the metal sulfides, TiO_2-based photocatalysts, and porous materials.

Synthesis with Metal Sulfide Catalysts

Lahiry and Haldar [29] demonstrated that NBD could be isomerized over some semiconductors, such as ZnO, ZnS, and CdS, under solar or high-pressure mercury lamp irradiation in the presence of air. Whereas ZnO did not show any side reaction, such as the formation of NBD dimers, ZnS and CdS produced a small amount of sulfur because of photocorrosion. Interestingly, all catalysts catalyzed the photoisomerization reaction only in the presence of oxygen, which means oxygen played an important role in the photocatalytic process [30]. Photogenerated electrons produced in the semiconductor's conduction band may convert oxygen into a superoxide radical anion, and the positive photogenerated hole produced may draw electrons from NBD, thereby forming the dirradicaloid of NBD. This species is then converted into QC. Extra photogenerated holes may combine with superoxide radical anions to revert to oxygen [31]. However, this mechanism does not explore the cation radical of NBD, and more detailed mechanisms still need to be explored further.

Hydrobenzoin has a wide range of applications in the field of fine chemicals and fuel synthesis. The compound is produced by the C–C coupling of benzaldehyde, which is formed by the dehydrogenation or partial oxidation of benzyl alcohol. The synthesis of hydrobenzoin from benzaldehyde usually requires the participation of reducing agents, but the direct preparation of hydrobenzoin from benzyl alcohol can avoid the use of reducing agents and reduce the number of reaction steps. Therefore, from the viewpoint of green and sustainable chemistry, the direct production of hydrobenzoin from benzyl alcohol is a simple and atomically economical method [32, 33].

Han et al. [34] reported the utilization of $ZnIn_2S_4$ nanosheets for the photocatalytic C–C coupling reactions of benzyl alcohols under blue LED irradiation with high conversion and selectivity (87–99% yield, 6 h). In the proposed mechanism of the photocatalytic C–C coupling reactions (Fig. 6a), benzyl alcohol is oxidized and deprotonated by the photogenerated h^+ of $ZnIn_2S_4$ to form ketyl radicals under visible light irradiation. These radicals are further converted to benzaldehyde after subsequent oxidation and deprotonation. The nanosheet morphology of $ZnIn_2S_4$ allows the rapid migration of excitons to the photocatalyst surface. However, the newly formed benzaldehyde on the catalyst surface may be reduced back to ketyl radicals because the excited e^- of $ZnIn_2S_4$ has sufficient reducing force. Dimerization of the in situ generated ketyl radicals generates hydrobenzoin, which can be consumed via two routes: (i) oxidation and deprotonation to produce benzoin or (ii) dehydration to form deoxybenzoin. Yuan et al. [35] prepared cetyltrimethylammonium bromide (CTAB) functionalized $ZnIn_2S_4$ monodisperse microflowers possessing efficient CO_2–CO conversion and high photocatalytic C–C coupling performance (99% conversion, 7 h) (Fig. 6b, c). The CTAB chain molecules act as structure-oriented mediators to induce surface and crystalline defects in $ZnIn_2S_4$; these defects are crucial in regulating the band structure and enhancing the charge carrier separation and transfer of ZIS. Bai et al. [36] prepared polyethylene glycol-modified $ZnIn_2S_4$ through the hydrothermal method (Fig. 6d) and demonstrated the high photocatalytic C–C coupling performance of the products (92.2% conversion, 92.9% selectivity, 6 h). Compared with traditional methods for the preparation of vicinal diols, the radical coupling of benzylic alcohols driven by visible light is a more convenient, efficient, and atomically economic route. Sulfide materials exposed to light for long periods stimulate the corrosion of holes. During this period, surface sulfide ions are easily oxidized, resulting in the deactivation of the photocatalyst. In this case, attention should be paid to the effect of the released sulfate or sulfur on the reaction process.

Synthesis with TiO_2-Based Photocatalysts

TiO_2 is the most widely used photocatalyst currently available because of its low cost, non-toxicity, and photostability [37]; given these properties, it has also been used in the photoisomerization of NBD to QC. Although the activity of TiO_2 is considered low on account of its low light absorption and high charge–hole recombination rate, several methods, such as doping and preparation of highly dispersed Ti–O materials, have been established to increase its photoactivity.

Doping with ions is regarded as an effective method to improve the visible light response, charge separation

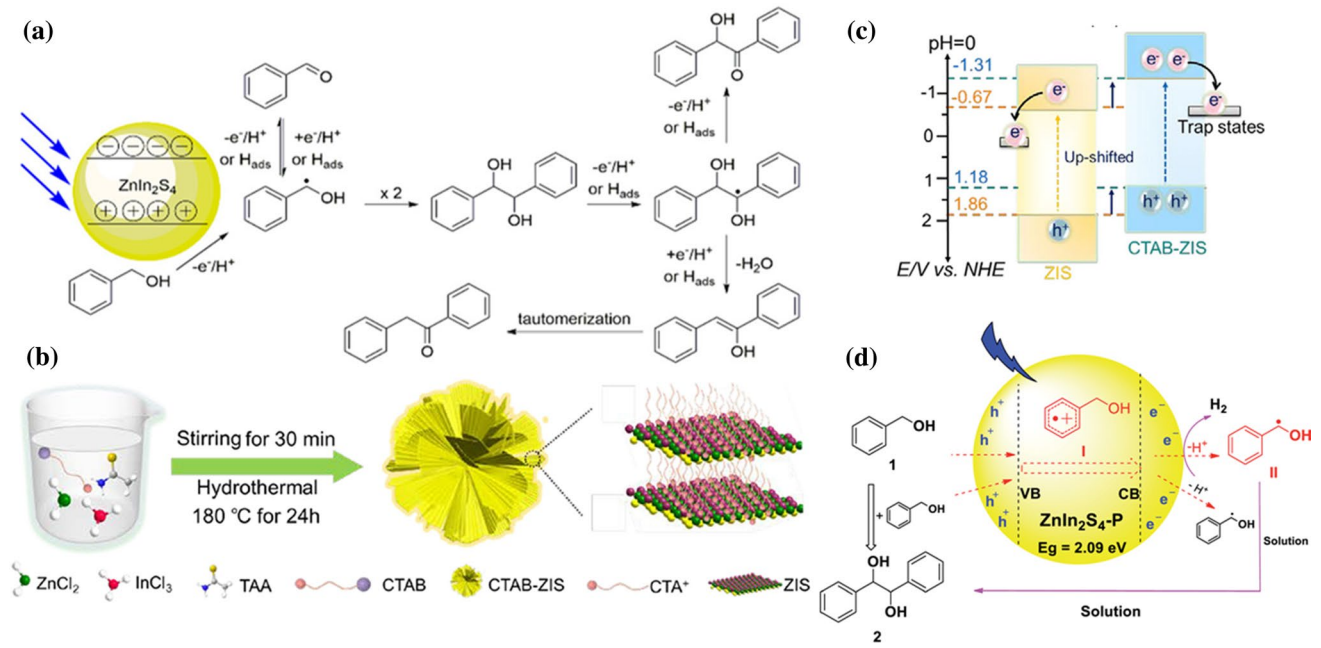

Fig. 6 **a** Proposed reaction pathways from benzyl alcohol to benzoin and deoxybenzoin. Reproduced with permission from Ref. [34]. Copyright 2020 American Chemical Society. **b** Flowchart for the fabrication of CTAB-ZIS (TAA = thioacetamide). **c** Schematic illustration of the band structures of ZIS and CTAB-ZIS. **b** and **c** are reproduced with permission from Ref. [35]. Copyright 2020 Elsevier. **d** Proposed reaction mechanism for the photocatalytic radical coupling of benzyl alcohol. Reproduced with permission from Ref. [36]. Copyright 2020 The Royal Society of Chemistry

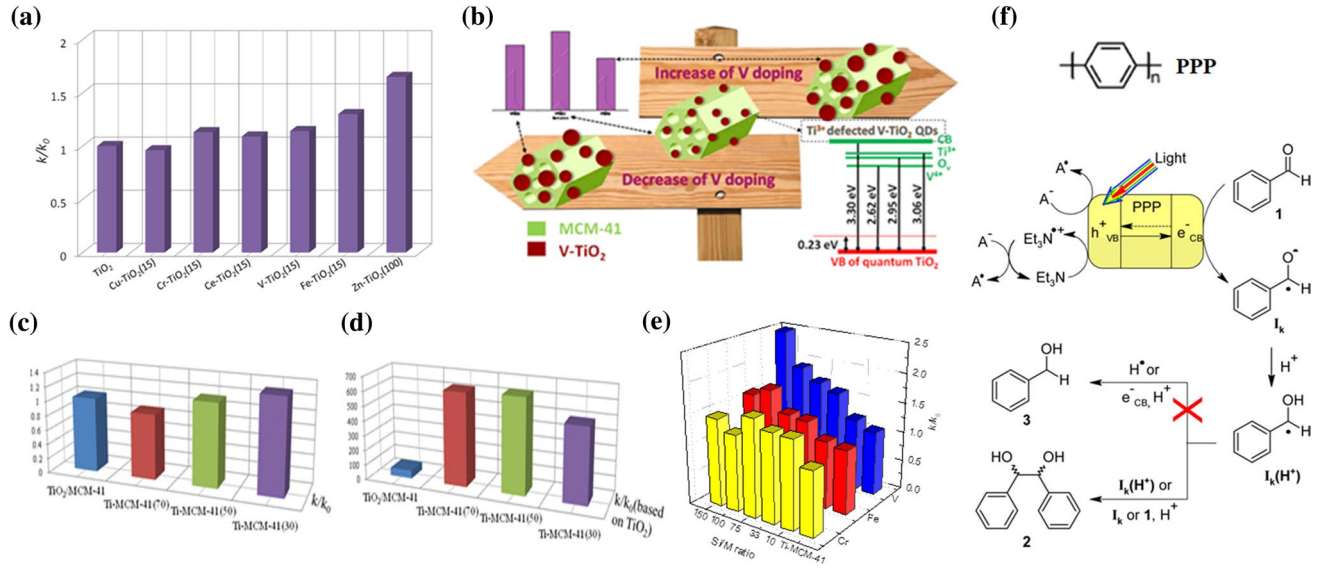

Fig. 7 **a** Activity of metal-doped TiO_2 for the photoisomerization of norbornadiene (NBD). Reproduced with permission from Ref. [39]. Copyright 2012 IntechOpen. **b** Effects of V-doping amount on the crystal size of TiO_2. Reproduced with permission from Ref. [41]. Copyright 2014 Royal Society of Chemistry. **c**, **d** Activity of Ti-MCM-41 and TiO_2-MCM-41 for the photoisomerization of NBD. Reproduced with permission from Ref. [39]. Copyright 2012 IntechOpen. **e** Activity of M (V, Fe, and Cr)-Ti-MCM-41 for the photoisomerization of NBD. Reproduced with permission from Ref. [47]. Copyright 2020 John Wiley and Sons. **f** Proposed mechanism of the PPP photocatalytic system in acid. Reproduced with permission from Ref. [59]. Copyright 2012 Elsevier

efficiency, and photoactivity of TiO_2 [38]. Zou's group [39, 40] prepared different metal-doped TiO_2 for the photoisomerization of NBD. The photocatalytic activities of various metal-doped TiO_2 (k/k_0) are shown in Fig. 7a. Doping with Cr, Ce, V, Fe, and Zn positively affected the photoisomerization of NBD; Zn-TiO_2 and Fe-TiO_2, in particular, showed high activity. Photogenerated charge transfer and separation are highly likely to occur through the M–O–Ti structure, in which the metal ion dopants mainly serve as activity centers. Surface lattice oxygen trapping with h^+ may serve as active sites for the photoisomerization of NBD, which produces Ti^{4+}–$[O^{2-}]_{lattice}$–Ti^{4+}–O^-⋯ NBD as an intermediate.

Zou's group [41] combined V-doping and other loading strategies to fabricate V-doped Ti^{3+}–TiO_2 QDs via hydrolysis using MCM-41 as a support. Trace V-doping decreased the TiO_2 crystal size, but higher V contents inversely increased the particle size (Fig. 7b). Moreover, a large amount of Ti^{3+} was simultaneously incorporated into the TiO_2 QDs, consistent with previous research. Among the V-doped TiO_2/MCM-41 (VTM) samples generated, the reaction rate of VTM20 was better than that of the original TiO_2/MCM-41 in the photoisomerization of NBD to QC (1.9 times). This effect is attributed to enhancements in charge separation efficiency caused by the quantum size and new defect- and dopant-mediated band levels.

Facet is a very important characteristic of crystalline materials. Different facets have different atomic and electronic structures, resulting in different physical and chemical properties. Wu et al. [42] prepared a series of TiO_2 materials with different facets to catalyze the C–C coupling of benzyl alcohol under visible light (99% yield, 2 h). This study revealed that the facet-dependent density of oxygen vacancies has a regulatory effect on the charge distribution and adsorption strength of surface species, thereby changing the overall selectivity of the product. Strong interactions between oxygen-rich-vacancy surfaces and the aldehyde lead to the preferential formation of CH–O· intermediates, and the strong adsorption of the intermediate promotes the subsequent addition of a second H atom to form alcohols. Furthermore, the ·C–OH intermediate is formed on the surface without oxygen vacancies, and the weak adsorption of the free radical intermediate allows it to desorb, resulting in subsequent C–C coupling.

Despite the advantages of the utilization of TiO_2-based photocatalysts in the photocatalytic synthesis of high-energy-density fuel, some drawbacks impede their practical photocatalytic applications. These drawbacks include a wide band gap, which may reduce the absorption of visible light, and rapid charge carrier recombination, which can reduce the number of electrons and holes available during the photocatalytic reaction.

Synthesis with Porous Catalysts

Besides common semiconductors, modified zeolites and molecular sieves also show catalytic activity for the photoisomerization of NBD. Ghandi et al. [43] prepared heavy atom (e.g., K^+, Cs^+, Tl^+)-exchanged Y zeolites to catalyze the intramolecular addition of some dienes, such as NBD, and obtained the corresponding triplet products. The porous structure of the zeolite–guest complex system apparently decreases the mobility of diene within the zeolite, which, in turn, increases energy transfer between the diene and heavy atom cation. This microreactor provides a constrained space to induce physical or chemical effects to achieve the required photoisomerization reaction [44].

Gu and Liu [45] synthesized La-, Cs-, Zn-, and K-exchanged Y zeolites for the photoisomerization of NBD to QC and revealed that the activity of the zeolites shows the order LaY (t) > LaY > CsY > ZnY > KY. The observed increase in activity was attributed to the heavy atom effect induced by spin–orbit coupling, which facilitates the transfer of the triplet state to the ground state. Among the four metals explored, La was the largest atom and, thus, demonstrated the highest activity. K-, Zn-, and Cs-exchanged Y zeolites resulted in Lewis acid sites, while La-exchanged Y zeolites generated Brönsted acid sites, which may also accelerate the valence isomerization of NBD to QC.

MCM-41 features well-defined hexagonal mesopores with a large internal surface area and, thus, exhibits great potential as supporting material for TiO_2 [46]. Incorporating Ti ions into the MCM-41 framework or loading on the walls of the latter has been reported to generate unique photocatalytic activity. Zou's group [47] prepared Ti-incorporated and Ti-loaded MCM-41 materials for the photoisomerization of NBD to QC. Incorporating Ti ions into the MCM-41 framework slightly affected the structural integrity of MCM-41, but the ordered structure was well maintained. The overall activity of the obtained products for the photoisomerization of NBD is shown in Fig. 7c, d. Given the different contents of Ti species in these materials, the photoisomerization activity based on TiO_2 was also calculated to compare the inherent activity of different catalysts, as shown in Fig. 7d. Considering the local structure of Ti, framework Ti species were most active, followed by polymerized species and then bulk TiO_2.

Transition metal-incorporated MCM-41 generally shows high photocatalytic activity due to the high dispersion of photoactive sites and separation efficiency of photogenerated carriers. Because Ti-MCM-41 exhibits high photoactivity for the isomerization of NBD, some scholars expect that incorporating a second transition metal ion into Ti-MCM-41 would further enhance its activity. Zou's group [48] synthesized a series of transition metal-incorporated (i.e., V, Fe, Cr) Ti-MCM-41 with a Si/Ti ratio of 30 for

the photoisomerization of NBD. At low metal incorporation contents, V^{5+} and Fe^{3+} were well-dispersed in the Si–O framework of MCM-41 with tetrahedral coordination. Increasing the metal content, however, resulted in the appearance of some species with higher coordination or even polymerized environments, as well as a slight weakening of the ordered structure. Cr ions were challenging to incorporate into the Si–O framework because of the formation of various species, such as Cr^{6+} and bulk oxides. All of the transition metal-incorporated Ti-MCM-41 samples showed higher activity compared with Ti-MCM-41 (Fig. 7e); in particular, V-Ti-MCM-41(150) exhibited remarkably high activity [49]. The photoisomerization activity observed was independent of the content of secondary transition metal ions, and enhancements in activity appeared to be related to the state of dispersion of these ions and the local structure. The highly ordered structure and large surface area of V-Ti-MCM-41(150) provide more active sites that could participate in the increased adsorption of NBD molecules.

Conjugated polymers are a series of organic materials with the delocalized π-conjugated systems and broad application prospects in photocatalytic transformations, such as photocatalytic H_2 evolution [50, 51], CO_2 reduction [52, 53], pollutant removal [54–57], and organic synthesis [58]. Rouch et al. [59] prepared the conjugated polymer poly-(*p*-phenylene) via the Yamamoto coupling reaction (Fig. 7f). The obtained polymer exhibited a suitable band structure with visible light absorption and could catalyze the photocatalytic C–C coupling of benzyl alcohol in the presence of Brønsted acids. Considering that the easily tunable chemical and optoelectronic structures enabled by synthetic protocols, various types of conjugated polymers could be obtained to meet the various demands of different photocatalytic synthesis methods for high-energy-density fuels.

Summary and Perspective

High-energy-density hydrocarbon fuel is an important propellant component that could improve the performance of aircraft, missiles, rocket propellers, and satellite control. Photocatalytic cycloaddition and C–C coupling reactions provide versatile and straightforward approaches to synthesize high-energy-density hydrocarbon fuels. In this review, we summarized the progress of research on high-energy-density fuel synthesis via the photocatalytic approach with a special focus on the relevant catalysts and mechanisms. Although conventional photocatalytic fuel synthesis procedures are generally eco-friendly and sustainable, their drawbacks, which include moderate conversion and selectivity, limit their applications. Therefore, researchers may wish to consider the following directions in future work:

(1) The goal of achieving high-energy-density fuel through efficient photosynthesis is developing more structures and synthetic methods to construct photocatalysts with high activity, selectivity, and stability. Single-atom catalysts continue to draw research interest because of their outstanding performance in catalysis; these catalysts can not only reduce the utilization of precious metals but also improve the catalytic activity of the reaction system. These 2D materials possess the unique ability to confine electrons to their ultrathin layer, resulting in exceptional optical and electronic properties. Moreover, 2D architectures lead to a large specific surface area, which enables surface reactions, such as the photocatalytic synthesis of high-energy-density fuel. Photocatalytic transformations are often accompanied by non-selective oxidation on account of the presence of highly oxidizing radicals. High selectivity toward the target compounds may be achieved by carefully tailoring the band structure according to the composition and structure of the photocatalyst.

(2) Developing more structures and reactions with which to construct fuel molecules with outstanding features, such as high density and low freezing point, is an important endeavor. Chain and branched-chain substituted monocyclic alkane fuels exhibit good low-temperature performance, but their density is quite low. By contrast, bicycloalkane and polycycloalkane fuels have higher densities, but their low-temperature properties are relatively poor. Spiro-ring molecules have a compact structure, high density, and good low-temperature performance. Thus, designing and synthesizing fuel molecules combining bridged-ring and spiro-ring framework structures may yield products with remarkably improved fuel density and low-temperature performance.

(3) Quantum chemical calculations can help researchers understand the nature of photosynthetic reactions and provide theoretical support for the design of high-energy density-fuel molecules. High-throughput computational simulations represent a powerful means to design new high-energy-density fuels. The group contribution method, in combination with first-principles quantum mechanics calculations, can quickly predict the physical, chemical, and energetic properties of various fuel molecules. Theoretical calculations can hasten the search for new hydrocarbon structures as next-generation high-performance fuels to meet the development needs of aviation and space technology. Moreover, such calculations enable further studies on catalytic mechanisms and structure–activity relationships. The available research mainly analyzes mechanisms by capturing active species but lack deep theoretical explanations to explain the actual process. The

knowledge provided by theoretical analyses can help reveal the complete details of these reaction mechanisms.

Acknowledgements The research was financially supported by the National Natural Science Foundation of China (Nos. 22161142002 and 21978200).

References

1. Zhao YF, Gao W, Li SW et al (2019) Solar-versus thermal-driven catalysis for energy conversion. Joule 3(4):920–937
2. Pan L, Ai MH, Huang CY et al (2020) Manipulating spin polarization of titanium dioxide for efficient photocatalysis. Nat Commun 11(1):1–9
3. Meng XG, Liu LQ, Ouyang SX et al (2016) Nanometals for solar-to-chemical energy conversion: from semiconductor-based photocatalysis to plasmon-mediated photocatalysis and photothermocatalysis. Adv Mater 28(32):6781–6803
4. Li R, Ma BC, Huang W et al (2017) Photocatalytic regioselective and stereoselective [2 + 2] cycloaddition of styrene derivatives using a heterogeneous organic photocatalyst. ACS Catal 7(5):3097–3101
5. Zhang XW, Pan L, Wang L et al (2018) Review on synthesis and properties of high-energy-density liquid fuels: hydrocarbons, nanofluids and energetic ionic liquids. Chem Eng Sci 180:95–125
6. Muldoon JA, Harvey BG (2020) Bio-based cycloalkanes: the missing link to high-performance sustainable jet fuels. Chemsuschem 13(22):5777–5807
7. Cuppoletti A, Dinnocenzo JP, Goodman JL et al (1999) Bond-coupled electron transfer reactions: photoisomerization of norbornadiene to quadricyclane. J Phys Chem A 103(51):11253–11256
8. Hammond GS, Wyatt P, DeBoer CD et al (1964) Photosensitized isomerization involving saturated centers. J Am Chem Soc 86(12):2532–2533
9. Gorman AA, Hamblett I, McNeeney SP (1990) Sensitization of the norbornadiene to quadricyclene conversion by substituted benzophenones: evidence against biradical intermediacy. Photochem Photobiol 51(2):145–149
10. Pan L, Feng R, Peng H et al (2014) A solar-energy-derived strained hydrocarbon as an energetic hypergolic fuel. RSC Adv 4(92):50998–51001
11. Shen C, Shang MJ, Zhang H et al (2020) A UV-LEDs based photomicroreactor for mechanistic insights and kinetic studies in the norbornadiene photoisomerization. AIChE J 66(2):e16841
12. Fife DJ, Moore WM, Morse KW (1985) Photosensitized isomerization of norbornadiene to quadricyclane with (arylphosphine) copper(I) halides. J Am Chem Soc 107(24):7077–7083
13. Trecker DJ, Foote RS, Henry JP et al (1966) Photochemical reactions of metal-complexed olefins: II—dimerization of norbornene and derivatives. J Am Chem Soc 88(13):3021–3026
14. Schwendiman DP, Kutal C (1977) Catalytic role of copper(I) in the photoassisted valence isomerization of norbornadiene. J Am Chem Soc 99(17):5677–5682
15. Sluggett GW, Turro NJ, Roth HD (1997) Rh(III)-photosensitized interconversion of norbornadiene and quadricyclane. J Phys Chem A 101(47):8834–8838
16. Franceschi F, Guardigli M, Solari E et al (1997) Designing copper(I) photosensitizers for the norbornadiene−quadricyclane transformation using visible light: an improved solar energy storage system. Inorg Chem 36(18):4099–4107
17. Rosi M, Sgamellotti A, Franceschi F et al (1999) Use of norbornadiene in solar energy storage: theoretical study of a copper(I) photosensitizer for the norbornadiene–quadricyclane transformation. Inorg Chem 38(7):1520–1522
18. Xie JJ, Pan L, Nie GK et al (2019) Photoinduced cycloaddition of biomass derivatives to obtain high-performance spiro-fuel. Green Chem 21(21):5886–5895
19. Xie JJ, Zhang XW, Shi CX et al (2020) Self-photosensitized [2 + 2] cycloaddition for synthesis of high-energy-density fuels. Sustain Energy Fuels 4(2):911–920
20. Marchand AP, Allen RW (1974) Improved synthesis of pentacyclo[5.4.0.02, 6.03, 10.05, 9]undecane. J Org Chem 39(11):1596
21. Singh VK, Raju BNS, Deota PT (1986) A convenient synthesis of novel pentacyclo[5.4.0.0^{2,6}.0^{3,10}.0^{5,9}]undecane-8,11-dione-4-spiro-1-cyclopropane. Synth Commun 16(13):1731–1735
22. Shi YJ, Jiang JY, Ma L et al (2017) Synthesis of 4,4'-bipentacyclo[5.4.0.0^{2,6}.0^{3,10}.0^{5,9}]undecane. Tetrahedron Lett 58(14):1376–1378
23. Shi YJ, Jiang JY, Wang JZ et al (2015) Synthesis of 4,4'-spirobi [pentacyclo[5.4.0.02,6.03,10.05,9]undecane]. Tetrahedron Lett 56(48):6704–6706
24. Underwood GR, Ramamoorthy B (1970) Chemical studies of caged compounds: the synthesis of hexacyclo[5,4,0,0^{2,6},0^{3,10},0^{5,9},0^{8,11}]undecane, "homopentaprismane." J Chem Soc D 1:12b–113
25. Eaton PE, Cassar L, Hudson RA et al (1976) Synthesis of homopentaprismane and homohypostrophene and some comments on the mechanism of metal ion catalyzed rearrangements of polycyclic compounds. J Org Chem 41(8):1445–1448
26. Eaton PE (1992) Cubanes: starting materials for the chemistry of the 1990s and the new century. Angew Chem Int Ed Engl 31(11):1421–1436
27. Gleiter R, Karcher M (1988) Synthesis and properties of a bridged *syn*-tricyclo[4.2.0.0^{2,5}]octa-3,7-diene: formation of propella[3$_4$] prismane. Angew Chem Int Ed 27(6):840–841
28. Maier G, Pfriem S, Schäfer U et al (1978) Tetra-tert-butyltetrahedrane. Angew Chem Int Ed 17(7):520–521
29. Lahiry S, Haldar C (1986) Use of semiconductor materials as sensitizers in a photochemical energy storage reaction, norbornadiene to quadricyclane. Sol Energy 37(1):71–73
30. Draper AM, de Mayo P (1986) Surface photochemistry: semiconductor photoinduced valence isomerization of quadricyclane to norbornadiene. Tetrahedron Lett 27(51):6157–6160
31. Li JY, Li YH, Qi MY et al (2020) Selective organic transformations over cadmium sulfide-based photocatalysts. ACS Catal 10(11):6262–6280
32. Lin Q, Li YH, Tang ZR et al (2020) Valorization of biomass-derived platform molecules via photoredox sustainable catalysis. Trans Tianjin Univ 26(5):325–340

33. Li YH, Li JY, Xu YJ (2021) Bimetallic nanoparticles as cocatalysts for versatile photoredox catalysis. EnergyChem 3(1):100047
34. Han G, Liu X, Cao Z et al (2020) Photocatalytic pinacol C–C coupling and jet fuel precursor production on $ZnIn_2S_4$ nanosheets. ACS Catal 10(16):9346–9355
35. Yuan L, Li YH, Tang ZR et al (2020) Defect-promoted visible light-driven CC coupling reactions pairing with CO_2 reduction. J Catal 390:244–250
36. Bai P, Tong XL, Gao YQ et al (2020) Visible light-driven selective carbon-carbon bond formation for the production of vicinal diols. Sustain Energy Fuels 4(11):5488–5492
37. Xiao J, Luo Y, Yang Z et al (2018) Synergistic design for enhancing solar-to-hydrogen conversion over a TiO_2-based ternary hybrid. Catal Sci Technol 8(9):2477–2487
38. Zou JJ, Zhu B, Wang L et al (2008) Zn- and La-modified TiO_2 photocatalysts for the isomerization of norbornadiene to quadricyclane. J Mol Catal A Chem 286(1–2):63–69
39. Zou JJ, Pan L, Wang L et al (2012) Molecular photochemistry-various aspects. IntechOpen publishing, London, pp 41–62
40. Pan L, Zou JJ, Zhang XW et al (2010) Photoisomerization of norbornadiene to quadricyclane using transition metal doped TiO_2. Ind Eng Chem Res 49(18):8526–8531
41. Pan L, Wang SB, Zou JJ et al (2014) Ti^{3+}-defected and V-doped TiO_2 quantum dots loaded on MCM-41. Chem Commun 50(8):988–990
42. Wu XJ, Li JQ, Xie SJ et al (2020) Selectivity control in photocatalytic valorization of biomass-derived platform compounds by surface engineering of titanium oxide. Chem 6(11):3038–3053
43. Ghandi M, Rahimi A, Mashayekhi G (2006) Triplet photosensitization of myrcene and some dienes within zeolite Y through heavy atom effect. J Photochem Photobiol A Chem 181(1):56–59
44. Zhang F, Li YH, Qi MY et al (2021) Photothermal catalytic CO_2 reduction over nanomaterials. Chem Catal. https://doi.org/10.1016/j.checat.2021.01.003
45. Gu L, Liu F (2008) Photocatalytic isomerization of norbornadiene over Y zeolites. React Kinet Catal Lett 95(1):143–151
46. Shen GQ, Pan L, Zhang RR et al (2020) Low-spin-state hematite with superior adsorption of anionic contaminations for water purification. Adv Mater 32(11):1905988
47. Zou JJ, Zhang MY, Zhu B et al (2008) Isomerization of norbornadiene to quadricyclane using Ti-containing MCM-41 as photocatalysts. Catal Lett 124(1–2):139–145
48. Zou JJ, Liu Y, Pan L et al (2010) Photocatalytic isomerization of norbornadiene to quadricyclane over metal (V, Fe and Cr)-incorporated Ti-MCM-41. Appl Catal B: Environ 95(3–4):439–445
49. Zou JJ, Xie J, Liu Y et al (2020) Design and synthesis of high-energy-strained fuels for advanced propulsion. In: Zou JJ, Zhang XW, Pan L (eds) High-Energy-Density Fuels for Advanced Propulsion: Design and Synthesis. Wiley, New Jersey, USA, pp 149–239
50. Zhang XH, Wang XP, Xiao J et al (2017) Synthesis of 1,4-diethynylbenzene-based conjugated polymer photocatalysts and their enhanced visible/near-infrared-light-driven hydrogen production activity. J Catal 350:64–71
51. Xiang YG, Wang XP, Rao L et al (2018) Conjugated polymers with sequential fluorination for enhanced photocatalytic H_2 evolution via proton-coupled electron transfer. ACS Energy Lett 3(10):2544–2549
52. Wang SY, Hai X, Ding X et al (2020) Intermolecular cascaded π-conjugation channels for electron delivery powering CO_2 photoreduction. Nat Commun 11(1):1–9
53. Zhao YF, Waterhouse GIN, Chen GB et al (2019) Two-dimensional-related catalytic materials for solar-driven conversion of CO_x into valuable chemical feedstocks. Chem Soc Rev 48(7):1972–2010
54. Xiang YG, Zhang XH, Wang XP et al (2018) Molecular structure design of conjugated microporous poly(dibenzo[b, d]thiophene 5,5-dioxide) for optimized photocatalytic NO removal. J Catal 357:188–194
55. Hou HJ, Zhang XH, Huang DK et al (2017) Conjugated microporous poly(benzothiadiazole)/TiO_2 heterojunction for visible-light-driven H_2 production and pollutant removal. Appl Catal B Environ 203:563–571
56. Yu T, Liu Z, Ma J et al (2020) The photocatalytic oxidation of As(III) enhanced by surface alkalinized g-C_3N_4. Trans Tianjin Univ 26:40–48
57. Xu ZM, Cao JZ, Chen X et al (2021) Enhancing photocatalytic performance of NH_2-UIO66 by defective structural engineering. Trans Tianjin Univ 27:147–154
58. Xiao J, Liu XL, Pan L et al (2020) Heterogeneous photocatalytic organic transformation reactions using conjugated polymers-based materials. ACS Catal 10(20):12256–12283
59. Rouch WD, Zhang M, McCulla RD (2012) Conjugated polymers as photoredox catalysts: a new catalytic system using visible light to promote aryl aldehyde pinacol couplings. Tetrahedron Lett 53(37):4942–4945

Chengxiang Shi received her B.S. and Ph.D. degrees in College of Chemistry, Nankai University, in 2010 and 2015, respectively. She became a postdoctoral research fellow in School of Materials Science and Engineering, Nankai University, in 2016. Currently, she is an assistant professor at School of Chemical Engineering and Technology, Tianjin University. Her research interests focus on the design and synthesis of hierarchically porous materials and their applications in heterogeneous catalysis.

Ji-Jun Zou received his B.S., M.S., and Ph.D. degrees in chemical engineering from Tianjin University in 2000, 2002. and 2005, respectively. Then he became an assistant professor at School of Chemical Engineering and Technology, Tianjin University, and was promoted as full professor from 2013. His research interests mainly surround nanomaterials for photo/electrocatalysis, fuel processing, and biomass conversion. He has received several awards including Technological Leading Scholar of 10,000 Talent Project, Changjiang Young Scholar by MOE, National Excellent Young Scientist by NSFC, and National Excellent Doctoral Dissertation by MOE. He is also an Associate Editor of *RSC Advances*.